

NASA TECHNICAL NOTE



NASA TN D-4467

c.1

NASA TN D-4467



LOAN COPY: RETURN TO  
AFWL (WLIL-2)  
KIRTLAND AFB, N MEX

# MIXING AND REACTION STUDIES OF HYDRAZINE AND NITROGEN TETROXIDE USING PHOTOGRAPHIC AND SPECTRAL TECHNIQUES

*by Marshall C. Burrows*  
*Lewis Research Center*  
*Cleveland, Ohio*



MIXING AND REACTION STUDIES OF HYDRAZINE AND NITROGEN  
TETROXIDE USING PHOTOGRAPHIC  
AND SPECTRAL TECHNIQUES

By Marshall C. Burrows

Lewis Research Center  
Cleveland, Ohio

(Film supplement C-258 available on request)

NATIONAL AERONAUTICS AND SPACE ADMINISTRATION

---

For sale by the Clearinghouse for Federal Scientific and Technical Information  
Springfield, Virginia 22151 - CFSTI price \$3.00

## ABSTRACT

Distances required to atomize, mix, and react  $N_2H_4$  and  $N_2O_4$  were experimentally determined for a quadlet injector element. Atomization occurred in less than 1 inch (2.5 cm), and vaporizing  $NO_2$  extended downstream for 4 inches (10.2 cm) or less. Hottest gases were in the oxidant-rich zones; fuel-rich gases appeared to be influenced by the decomposition reaction of hydrazine. Concentration profiles of  $H_2O$  determined from total radiation and gas temperature compared favorably with  $H_2O$  concentrations calculated for combustion profiles limited by either fuel or oxidant vaporization.

Technical Film Supplement C-258 available on request.

# MIXING AND REACTION STUDIES OF HYDRAZINE AND NITROGEN TETROXIDE USING PHOTOGRAPHIC AND SPECTRAL TECHNIQUES \*

by Marshall C. Burrows

Lewis Research Center

## SUMMARY

Photographs, thermocouple measurements, and emission spectra were used to study the atomization, mixing, and reaction characteristics of hydrazine ( $N_2H_4$ ) and nitrogen tetroxide ( $N_2O_4$ ). The propellants were injected through a quadlet element into a 2-inch- (5.1-cm-) diameter combustor at an oxidant-fuel weight ratio of 1.0, a chamber pressure of approximately 19 atmospheres ( $19.25 \times 10^5 \text{ N/m}^2$ ), and a contraction ratio of 9.85. Propellant behavior was followed from the point of injection to the mixed product gases 18 inches (45.7 cm) downstream.

Atomization of the liquid propellants occurred in less than 1 inch (2.5 cm). Opaque pockets of nitrogen dioxide ( $NO_2$ ) extended from 2 to 4 inches (5.1 to 10.2 cm) downstream from the injection point. Fuel-injected sides of the chamber remained fuel rich with respect to the metered oxidant-fuel weight ratio; oxidant-injected sides of the chamber remained relatively oxidant rich. This behavior was attributed in part to interfacial or liquid-phase reactions that prevent appreciable jet interpenetration and mixing in the liquid phase.

The highest combustor temperature, when corrected for losses, is close to the calculated stoichiometric gas temperature of  $3160^\circ \text{K}$ ; the lowest temperatures are above the calculated temperature of  $1465^\circ \text{K}$  for the decomposition of hydrazine. Products were well mixed at downstream axial distances of 11 inches (27.9 cm) or more from the injector.

Photographic emission spectra from the gases near the injector were limited principally to the transparent gases on the fuel-injected sides of the combustor. Spectral radiation from the NH radical was concentrated close to the atomizing fuel jets and reached the maximum intensity 1 inch (2.5 cm) from the impingement point of the jets.

Measured gas temperatures and total radiation intensities were used with Planck's radiation law and a thin gas approximation to calculate the concentration profiles of water as a function of the axial downstream distance. Experimentally determined concentrations matched those determined for vaporization-limited combustion if the fuel-rich and oxidant-rich sides of the chamber were considered.

---

\* Published in AIAA J., vol. 5, no. 9, Sept. 1967, pp. 1700-1701.

## INTRODUCTION

Many researchers have considered the physical behavior of hydrazine ( $N_2H_4$ ) and nitrogen tetroxide ( $N_2O_4$ ) jets to be approximately described by nonreactive and nonmiscible liquids (refs. 1 to 3). However, if the hypergolic nature of these propellants causes the jets to be diverted away from the impingement point, the propellants will not mix and react in the short distances necessary for good performance and hardware design (refs. 4 to 6). A study of the physical behavior at the impingement point should therefore be coupled with an examination of the corresponding chemical behavior in this region.

Analytical studies of hydrazine - nitrogen tetroxide performance have been hampered by a lack of information of the effects of atomization, vaporization, and the decomposition reactions of both propellants (refs. 7 and 8). Ignition and gas phase kinetic reactions have been studied for this system, but corresponding studies in a high-pressure combustor with liquid phase injection have been lacking (refs. 9 and 10).

The purpose of this study was to obtain more information on the physical processes of atomization, vaporization, and mixing, as well as to determine from temperatures and emission spectra which controlling chemical processes take place. This information can serve to define a more accurate analytical model for the overall combustion of liquid hydrazine and liquid nitrogen tetroxide in a rocket combustion chamber.

Silhouette photographs were used to determine the chamber length required to atomize the impinging jets; to vaporize and react the optically dense nitrogen dioxide ( $NO_2$ ); and to observe time-varying processes near the impingement point. Tungsten - tungsten-rhenium thermocouples were used to determine the gas temperature profile as a function of the axial downstream distance. Spectral radiation bands of  $NH$ ,  $OH$ , and  $NH_2$  were used to determine apparent decomposition- and oxidation-reaction zones. Pyrometer measurements of total radiation due primarily to  $H_2O$  radiation were used to determine the extent of reaction as a function of the axial downstream distance. Experimentally determined  $H_2O$  concentrations were compared with those determined for vaporization-limited combustion.

The atomization, mixing, and extent of reaction produced by impinging jets of hydrazine and nitrogen tetroxide were photographed with a high-speed motion-picture camera. The film also shows the distances required to form ligaments and drops near the impingement point. Mixing and the extent of reaction can be determined from the disappearance of oxidizer and the formation of radiating transparent products.

A motion-picture supplement C-258 has been prepared and is available on loan. A request card and a description of the film are included at the back of this report.

# APPARATUS AND PROCEDURE

## Combustor

An impinging quadlet injector element was used for all combustor tests. The four tubes were positioned as shown in figures 1(c) and (d) with impingement at an included angle of  $90^\circ$  ( $45^\circ$  to the combustor axis) (figs. 1(a) and (b)). The inside diameter of each tube was  $0.068 \pm 0.001$  ( $0.175 \pm 0.003$  cm) inch, and the free stream length of each jet was less than 0.1 inch (0.25 cm) before impingement. The alinement of the tubes had a large effect on the axial symmetry of the spray pattern. Hence, the injector was inspected and the flow checked periodically with water to ensure constancy of test conditions.

All combustor parts except the nozzle were made of stainless steel to prevent surface reactions with the propellants and emission spectra from the metal oxides, especially copper. A copper nozzle was used because it maintained its dimensions better than stainless steel and did not introduce any copper-compound emission spectra. Run lengths were between 1.0 and 1.5 seconds, with equilibrium flow and chamber pressure

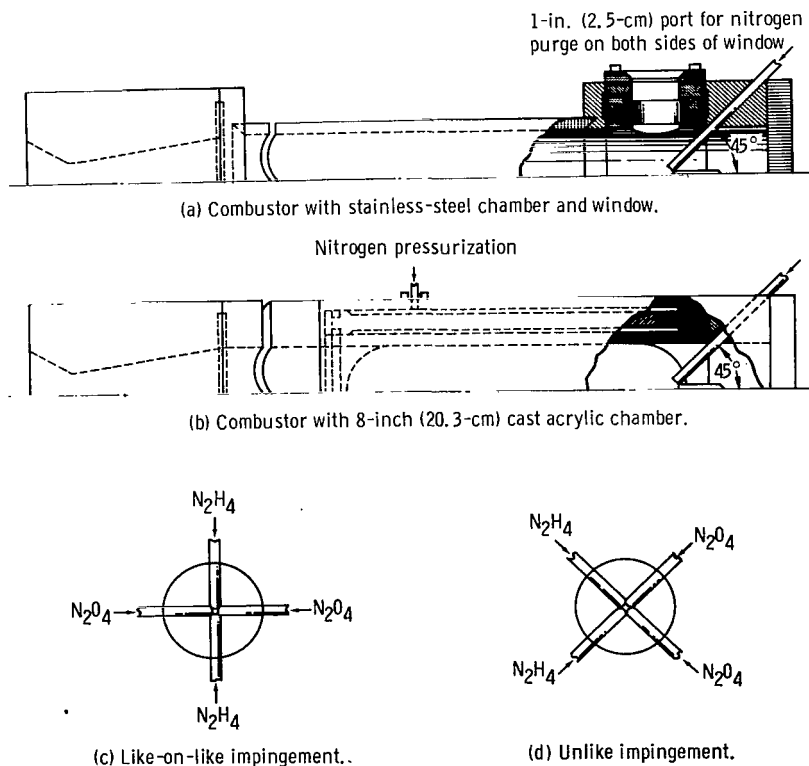


Figure 1. - Hydrazine - nitrogen tetroxide combustor. Inside diameters of four injector tubes, 0.068 inch (0.175 cm); angle of tubes to combustor axis,  $45^\circ$ ; chamber diameter, 2 inches (5.1 cm); chamber length, 20 inches (50.8 cm); nozzle diameter, 0.640 inch (1.625 cm); nozzle conical convergence, 3 inches (7.6 cm).

established at 0.2 second or less after ignition. The chamber pressure was 19 atmospheres ( $19.25 \times 10^5 \text{ N/m}^2$ ), the oxidant-fuel weight ratio was 1.0, and the contraction ratio was 9.85. At these conditions, the calculated jet velocity of the hydrazine was 95 feet per second (28.9 m/sec) and that of the nitrogen tetroxide was 64 feet per second (19.5 m/sec). Windowed or transparent plastic chamber sections permitted observation of the combustor gases from the impingement point to 18 inches (45.7 cm) downstream.

## Photographs

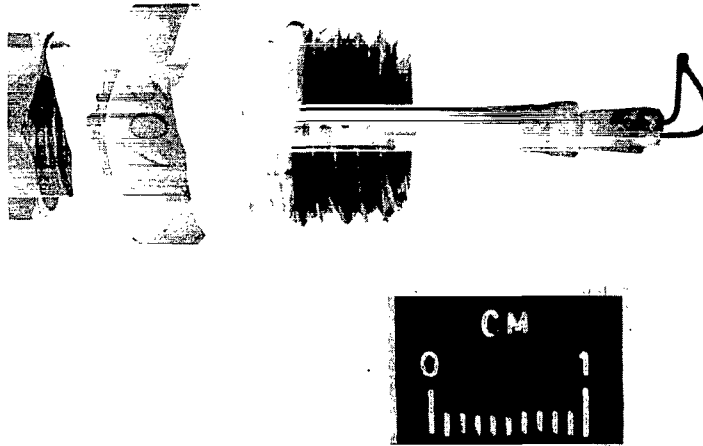
The illumination for silhouette photographs of the atomization zone was provided by a zirconium continuous arc source. Light passed through a converging lens and through the engine windows, and the spray to the rotating prism camera. The effective exposure time for these photographs was 33 microseconds at a rate of 6000 frames per second. High-speed tungsten-rated color film was used in the camera.

Photographic spectra of the combustor gases were obtained on a 35-millimeter film strip with the use of a 1.5-meter grating-spectrograph with quartz optics. A spectral slitwidth of approximately 0.002 micron was required for the 1.0-second exposure time. The shutter was programmed to open automatically in the middle of the combustor test run. The range of the spectrograph was 0.21 to 0.78 micron, but the spectral intensities within the combustor and the photographic film limitations reduced this range to approximately 0.25 to 0.65 micron.

## Other Instrumentation

Ultraviolet radiation intensities in the spectral range of 0.26 to 0.40 micron were measured with a bandpass photometer consisting of an absorption filter, a phototube with ultraviolet sensitivity, and an amplifier. A voltage-time recorder plotted the average ultraviolet radiation intensity as a function of time. Total radiation intensities were recorded in the same manner with a mirror-type pyrometer responding to infrared radiation between 0.8 and 3.5 microns.

Gas temperatures in the combustor were obtained from the thermovoltages generated by tungsten - tungsten-26-percent-rhenium bare wire thermocouples (fig. 2). The junctions were welded beads approximately twice the diameter of the 0.015-inch (0.032 cm) wires. The junction extended approximately 0.1 inch (0.25 cm) from the alumina and stainless-steel holder. Most of the thermocouple junctions withstood the combustion environment for at least one run, especially in the nonoxidizing (fuel-rich) gas zones. It is obvious that the oxidation of the junction itself could increase the apparent



C-67-4443

Figure 2. - Tungsten - tungsten-26-percent-rhenium thermocouple. Wire diameter, 0.015-inch (0.381-cm) alumina insulator; stainless-steel sheath.

temperature of the gases in oxidizer-rich zones. However, this reaction would be the most serious at mixture ratios greater than 1.5 and at temperatures above  $3000^{\circ}\text{K}$ .

Equilibrium thermocouple readings, taken on opposite sides of the chamber, were averaged if they agreed within 10 percent or they were repeated if their difference was larger (fig. 3). The thermocouple measurements were in error due to the effects of the junction radiation and thermal conduction of the thermocouple wires. A maximum error of  $300^{\circ}\text{K}$  in gas temperature will occur at an indicated gas temperature of  $2900^{\circ}\text{K}$  if the following assumptions are made: the combustor walls are  $1370^{\circ}\text{K}$ , the gases within the chamber are transparent, and the temperature of the thermocouple wire out-

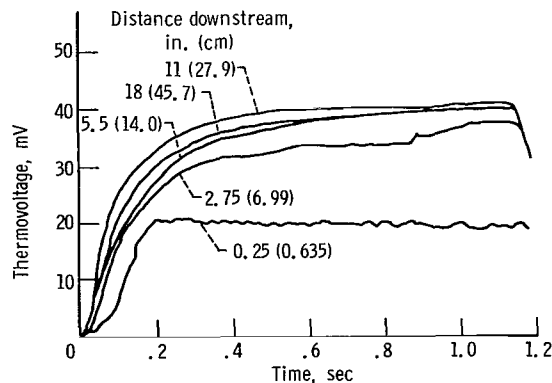


Figure 3. - Typical thermocouple voltage as function of run time. Readings taken 0.25 inch (0.635 cm) from combustor axis and at various downstream distances.

side the combustor is  $300^{\circ}$  K. The total error decreases to  $20^{\circ}$  K at an indicated temperature of  $2260^{\circ}$  K. Unfortunately, the exact error in temperatures caused by the radiation and conduction of the thermocouple cannot be determined; the aforementioned error was considered the maximum value.

## EXPERIMENTAL RESULTS

### Silhouette Photographs

Photographs were taken with either the windowed or plastic chamber in position between the injector element and the nozzle (fig. 4). These photographs showed that the

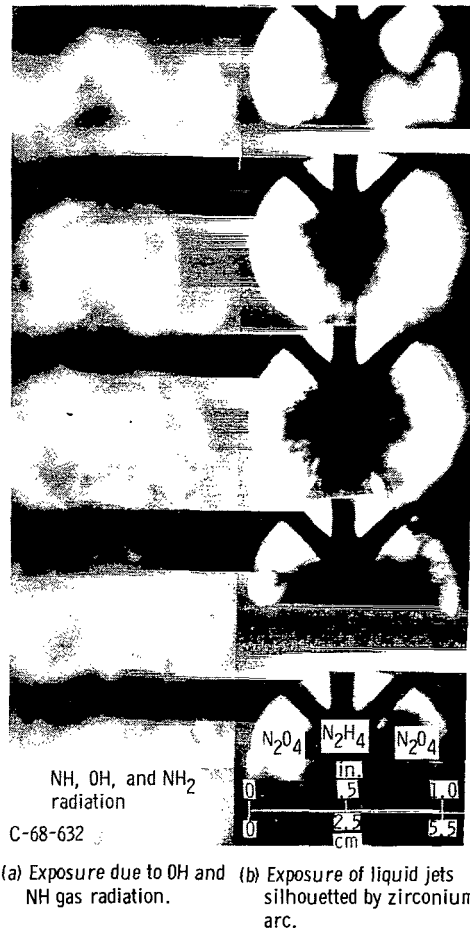


Figure 4. - Film sequence showing impinging of hydrazine and nitrogen tetroxide in windowed chamber. Film speed, 6000 frames per second; exposure time,  $33 \times 10^{-6}$  second at  $f/2.8$ .

atomization distance was not constant, but varied from 0.3 to 1.3 inches (0.8 to 3.3 cm) from the impingement point, with an average distance of less than 1 inch (2.5 cm). This variation was repetitive with a period of approximately 0.8 millisecond. Injection velocities of the  $N_2H_4$  and  $N_2O_4$  were not equal (95 and 64 ft/sec or 28.9 and 19.5 m/sec, respectively); and axial velocities of the impinging liquids, as measured from the photographs, appeared to vary within these limits. Some photographs showed dense oxidizer streams returning to the combustor walls at an angle of  $45^\circ$  to the axis of the combustor. This behavior prevented complete mixing with, or penetration of, the fuel by the oxidizer streams. Performance tests at the Jet Propulsion Laboratory (ref. 6) using much larger, unlike, impinging jets indicated similar behavior. At a mixture ratio of 1.0, the momentum of the fuel streams exceeded that of the oxidizer streams by nearly 50 percent. Liquid fuel therefore tended to occupy the core of the impingement zone with the oxidizer streams repelled from the fuel at their interfaces.

Dense pockets of  $NO_2$ , identified by their reddish-brown color, extended downstream for approximately 4 inches (10.2 cm) with velocities that ranged from 65 to 190 feet per second (19.8 to 57.8 m/sec), as seen in figure 5. Liquid  $N_2H_4$ , appearing as a gray area

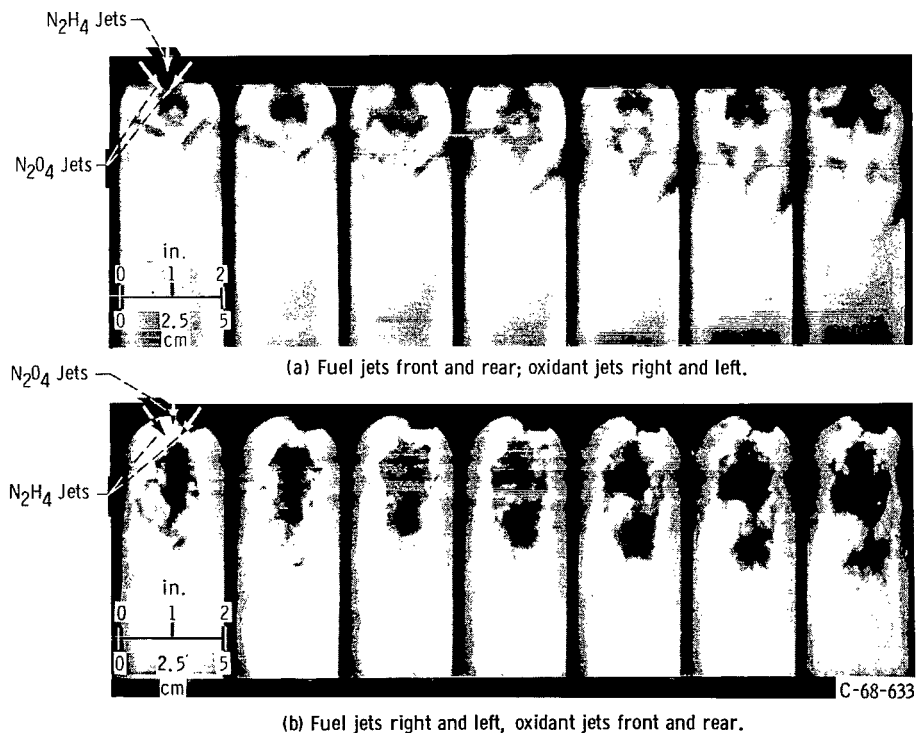


Figure 5. - Film sequence showing impinging jets of hydrazine and nitrogen tetroxide in transparent chamber. Film speed, 6000 frames per second; exposure time,  $33 \times 10^{-6}$  second at  $f/2.8$ .

near the impingement point, disappeared soon after atomization was completed, that is, 2 inches (5.1 cm) downstream.

### Thermocouple Measurements

Gas temperatures within the combustor, determined by tungsten - tungsten-26-percent-rhenium thermocouples, varied from  $1750^{\circ}\text{K}$  on the fuel-injected sides of the combustor to  $2910^{\circ}\text{K}$  on the oxidant-injected sides of the combustor, as shown in figure 6. Maximum combustor temperatures occurred on the oxidizer-injected sides from 2.75 to 5.5 inches (7.0 to 14.0 cm) from the impingement point. Temperatures on the fuel-injected sides were considerably lower; in the downstream positions, gases approached the temperatures of reacted and mixed products. The temperature profile across the chamber in the downstream positions showed that this temperature difference was the result of heat transfer to the combustor walls, radial variations in the oxidant-fuel weight ratio, or a combination of these factors. For example, a decrease of  $100^{\circ}\text{K}$  in the core temperature, from  $2760^{\circ}\text{K}$  at 11 inches (27.9 cm) downstream to  $2660^{\circ}\text{K}$  at

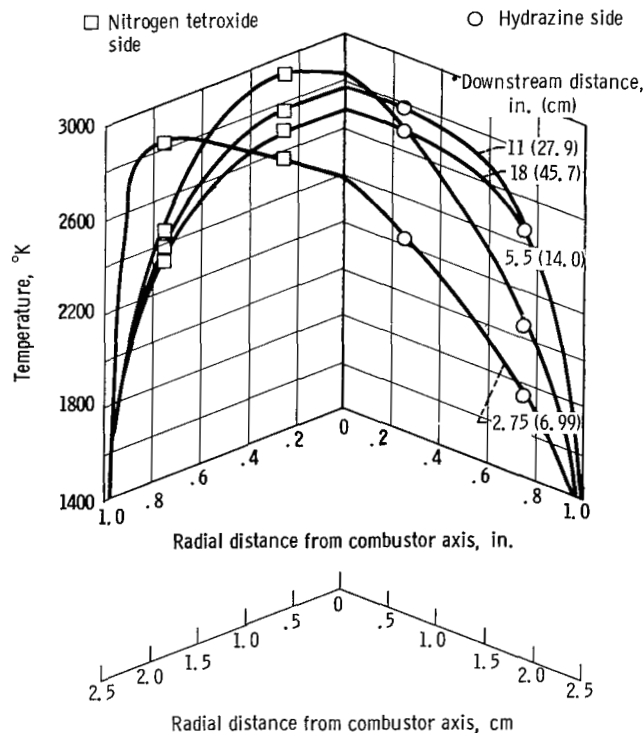
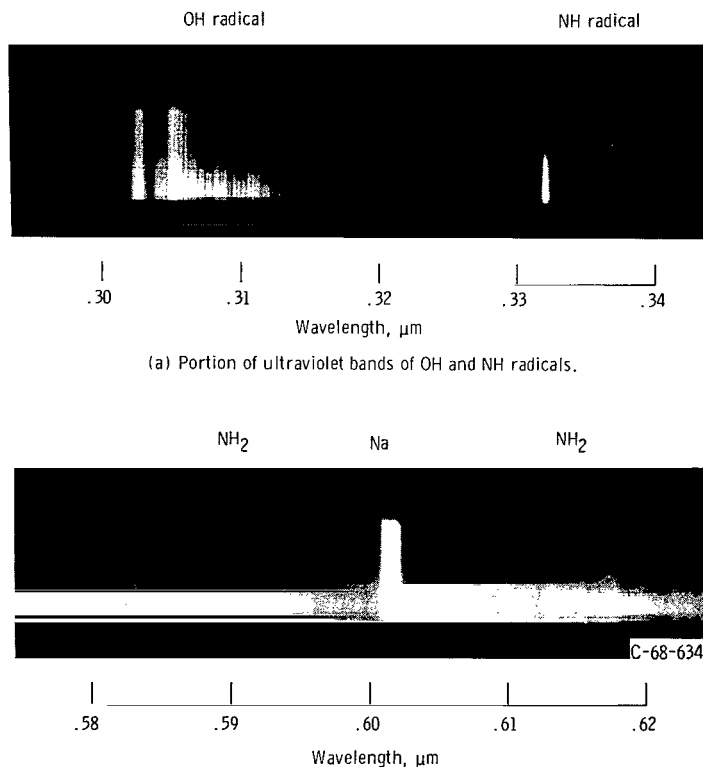


Figure 6. - Uncorrected gas temperature profile at various distances from the injector. Oxidant-fuel weight ratio, 1.0.

18 inches (45.7 cm) downstream can account for heat transfer of 1 Btu per square inch per second ( $1.63 \times 10^6 \text{ W/m}^2$ ) to the walls. As noted in figure 6, the gas temperatures derived from thermocouple measurements are uncorrected for radiation from the junction and conduction along the wires. Because of the low conductivity of tungsten and the exposure of 0.1 inch (0.25 cm) of thermocouple wire to the high-temperature gases, the major error in the thermocouple reading should be caused by radiation losses from the junction. The estimated maximum temperature correction would raise the maximum measured gas temperatures from  $2910^\circ$  to  $3210^\circ \text{ K}$ , or approximately  $50^\circ \text{ K}$  above the calculated temperature for equilibrium products obtained according to the calculation procedures outlined in reference 11.

### Photographic Spectra

Spectra of the gases in the combustor were obtained for the ultraviolet and visible wavelength spectra. Bands of the OH radical from 0.26 to 0.35 micron and bands of the



(a) Portion of ultraviolet bands of OH and NH radicals.

(b) Sodium D lines and portion of  $\text{NH}_2$  visible bands.

Figure 7. - Spectra from hydrazine - nitrogen tetroxide combustor gases at point of impingement. Film exposure time, 1 second at  $f/25$ .

NH radical centered at 0.336 and 0.337 micron were the principal radiating species in the ultraviolet range (fig. 7(a)). When either the photographic exposure or the slitwidth was increased considerably, the  $\text{NH}_2$  radiation bands from 0.50 to 0.70 micron were recorded (fig. 7(b)). Ultraviolet and visible radiation from the combustor gases were considerably more intense on the fuel-rich sides of the combustor. For example, the NH band at 0.336 micron reached a maximum intensity (corresponding to maximum density on the film) at a distance of 1 inch (2.5 cm) from the injector on the fuel-rich sides

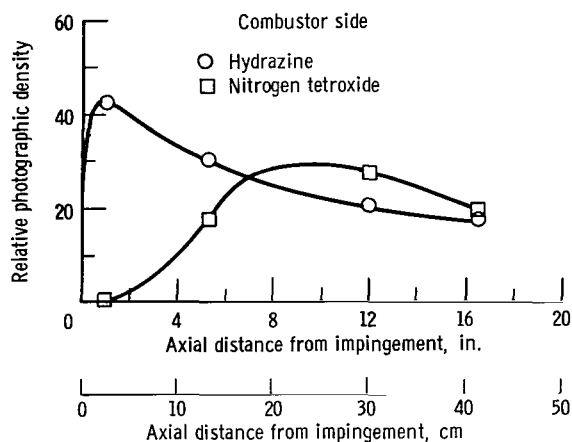


Figure 8. - Density of 0.336-micron NH radical spectral band as function of axial downstream distance. Oxidant-fuel weight ratio, 1.0; chamber pressure, 19 atmospheres ( $19.25 \times 10^5 \text{ N/m}^2$ ).

of the combustor shown in figure 8. Oxidizer-rich gases apparently absorbed most of the NH radiation near the injector.

### Photometer and Pyrometer Data

The ultraviolet OH bands and the infrared  $\text{H}_2\text{O}$  bands were considered the strongest spectral emitters in the combustor. A photometer and a pyrometer, respectively, were the most reliable means of recording their radiant intensities in terms of average output voltages. Figure 9 shows the photometer output as a function of the axial downstream distance from the injector. Ultraviolet emission from the gases increased in intensity with increasing axial distance and was consistently higher on the fuel-rich sides of the combustor, even though higher gas temperatures were recorded by the thermocouples in the oxidizer-rich gases. As in the case of NH, the OH radiation was attenuated by the oxidizer-rich gases.

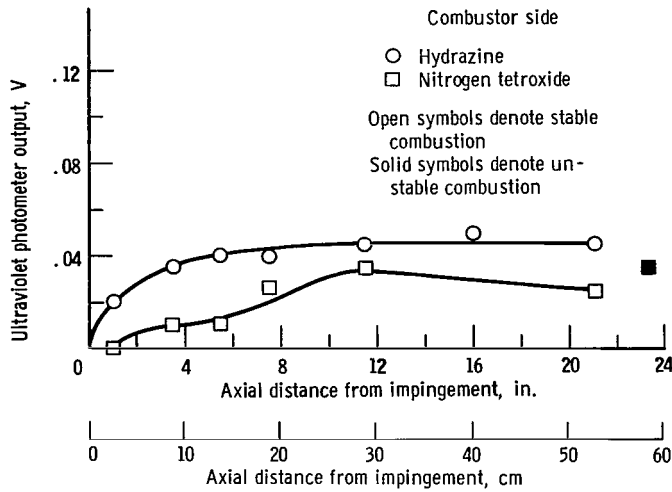


Figure 9. - Ultraviolet radiation as function of axial downstream distance. Principal emitter, OH radical; OH spectral band, 0.26 to 0.40 micron; oxidant-fuel weight ratio, 1.0; chamber pressure, 19 atmospheres ( $19.25 \times 10^5$  N/m<sup>2</sup>).

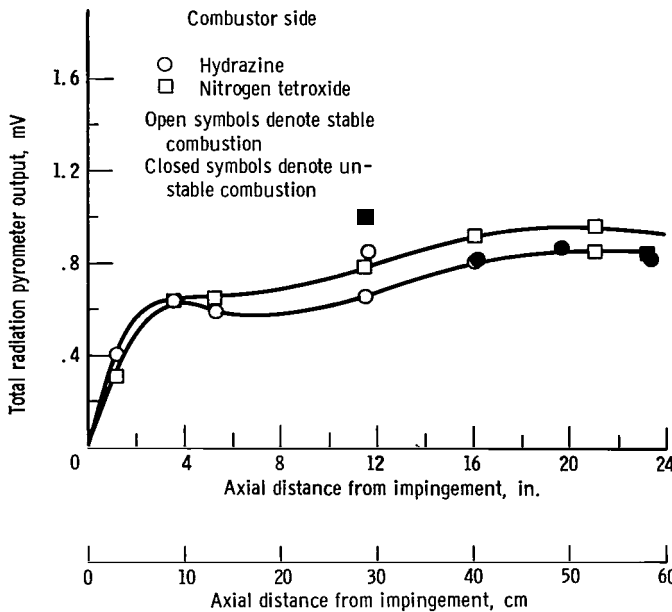


Figure 10. - Total radiation as function of axial distance. Principal emitter, water; water spectral bands at 0.9, 1.1, 1.4, 1.9, and 2.7 microns; oxidant-fuel weight ratio, 1.0; chamber pressure, 19 atmospheres ( $19.25 \times 10^5$  N/m<sup>2</sup>).

The output of the total radiation pyrometer is shown in figure 10 as a function of the axial downstream distance for the fuel-injected and the oxidizer-injected sides of the combustor. Radiant intensities increased rapidly for the first 4 inches (10.2 cm) from the injector and then slowly increased to final values that were close to the mixed equilibrium-product radiation. Total radiation from gases on the oxidizer-injected sides was consistently higher than that on the fuel-injected sides for most of the combustor length. This result is in contrast to that for the ultraviolet radiation where the ultraviolet radiation from gases was higher on the fuel-injected sides of the combustor.

Occasional combustor tests showed an oscillatory rather than a stable pressure environment with an amplitude as high as 50 percent of the chamber pressure. The mode of oscillation was identified as the first longitudinal mode. Generally, mixing was enhanced by the oscillatory burning, and the radiation intensities on the fuel-injected sides of the combustor became equal to those on the oxidizer-injected sides. The effect of this pressure environment is shown in figure 9 for the ultraviolet radiation data and in figure 10 for the total radiation data.

## DISCUSSION

Large density and temperature gradients within the combustor reduced the spatial resolution of the photographs in figure 4, and the 33-microsecond exposure time of each frame was too long to stop high-velocity droplets. However, the photographs did show the approximate end of propellant ligaments 0.3 to 1.3 inches (0.76 to 3.3 cm) from impingement point. Any liquid that extended beyond this distance should be in the form of individual droplets.

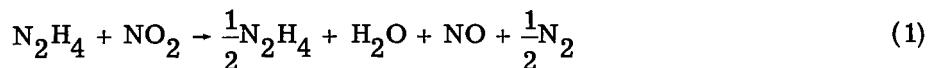
Based on the variation in injection velocities of the propellants, the average 1-inch (2.5-cm) atomization distance corresponds to a time of 0.9 to 1.3 milliseconds. It is perhaps fortuitous that these times bracket the minimum ignition delay observed for these propellants in the liquid phase in bomb tests of 1.2 milliseconds (ref. 12). Aside from this comparison, there did not appear to be any large, highly exothermic reaction upon impact of the fuel and oxidizer streams. Thermocouples placed at, or slightly below, the impingement point remained essentially at the temperature of the liquids. The only indication of immediate reaction between the fuel and the oxidizer was a repelling force they encountered at the impingement point. The jets, rather than forming a uniform propellant distribution, appeared to be repelled after contact and returned to the sides of the chamber from which they were injected.

The heat released by the interfacial reaction between hydrazine and nitrogen tetroxide is sufficient to overcome the momentum of impingement and to keep the oxidizer and fuel separated. With like propellant tubes opposed, as shown in figure 1(c), the con-

tact area between unlike propellants would not be a plane surface, but rather an irregular surface that is a function of the momentum ratio between the two propellants. A few combustor tests were made with like propellants in the adjacent tubes shown in figure 1(d). The combustor performance decreased considerably, and photographs showed extreme stratification of the propellants as they moved down the chamber on the same sides that they were injected. This is shown best in the film supplement C-258 available on loan and described at the back of this report. It was obvious that the injector arrangement of figure 1(c) provided a better distribution of the propellant streams.

A large number of possible reactions are available in the hydrazine - nitrogen tetroxide system. Ignition kinetics have been investigated by Skinner, et al. (ref. 9), and the steady-state behavior was studied in a reactor by Sawyer (ref. 10). In both studies, the decomposition of hydrazine formed an essential part of the overall reaction mechanism. The simple reaction  $\text{N}_2\text{H}_4 \rightarrow \text{N}_2 + 2\text{H}_2$  is not followed, but rather the more exothermic one:  $2\text{N}_2\text{H}_4 \rightarrow 2\text{NH}_3 + \text{H}_2$ . Decomposition of liquid hydrazine at  $298^\circ\text{K}$  therefore results in an equilibrium gas temperature of  $1465^\circ\text{K}$  for a heat of reaction of 23.1 kilocalories per mole (96.7 J/mole) of hydrazine. The lowest gas temperature measured in the combustor was  $1750^\circ\text{K}$  at 2.75 inches (6.99 cm) from the injector, which may correspond to fuel decomposition in that region. Decomposition of hydrazine was confirmed by the spectrogram of the emitting gases (fig. 8), which showed the emission of the NH and  $\text{NH}_2$  radicals in the fuel-rich zones immediately downstream of the injection point. These radicals are considered an initial product of the overall  $\text{N}_2\text{H}_4$  decomposition (ref. 13). Maximum NH radiation at 1 inch (2.5 cm) from the fuel side of the injector therefore indicates maximum decomposition of the hydrazine at the same point that atomization takes place.

The oxidation reactions in the combustor were coincident with, or they closely followed, the decomposition of the fuel, since OH radiation was always observed in regions that strongly emitted  $\text{NH}_2$  and NH. This observation is consistent with Sawyer's (ref. 10) proposed reaction mechanisms in which an initial step in the reaction of  $\text{N}_2\text{H}_4$  and  $\text{N}_2\text{O}_4$  is the formation of NO and OH. Hydrazine reacts further with NO and OH to form the final products  $\text{N}_2$  and  $\text{H}_2\text{O}$ . In terms of the overall reaction mechanism, the suggested oxidation reactions are





No emission bands due to NO or O<sub>2</sub> were observed in the emission spectra from the combustor. Since their wavelengths overlap those for OH, some emission bands could be masked by the very intense OH bands (ref. 14).

From the assumptions that the water vapor in the combustor always remains in thermal equilibrium and that its emission bands account for most of the infrared radiation, the water vapor concentration can be determined as a function of the axial distance downstream from the injector. The fuel-rich and oxidant-rich sides of the combustor must be considered separately because of the marked differences in their measured radiation and temperature profiles. The equilibrium concentration of H<sub>2</sub>O can be calculated from the equation

$$\frac{P_{\text{H}_2\text{O}}}{P_o} = \frac{I_G \lambda^5 T_G}{K L P_o T_o C_1} \left( e^{C_2/\lambda T_G} - 1 \right) \quad (4)$$

where

- $P_{\text{H}_2\text{O}}$  partial pressure of water vapor, atm; N/m<sup>2</sup>
- $P_o$  reference pressure of 19 atm;  $19.25 \times 10^5$  N/m<sup>2</sup>
- $I_G$  measured gas radiation
- $\lambda$  effective wavelength of water vapor radiation, assumed equal to 2.6  $\mu\text{m}$
- $T_G$  gas temperature taken as average of two thermocouple radial locations and corrected for maximum radiation loss
- $K$  constant that includes integrated absorption coefficient
- $L$  optical path length through combustor, assumed constant at 5 cm
- $T_o$  reference temperature of 2600<sup>o</sup> K
- $C_1, C_2$  constants in Planck's radiation law

The mole fraction of water vapor is assumed equal to 0.4 at 18 inches (45.7 cm) downstream and is the value calculated from equilibrium products at a fuel-oxidant weight ratio of 1.0 from reference 11. Equation (4) is valid for gases with a low emissivity, that is, a thin gas approximation.

Concentration profiles of the water vapor were plotted as a function of the axial downstream distance in figure 11. On the fuel-rich sides of the combustor, the maximum

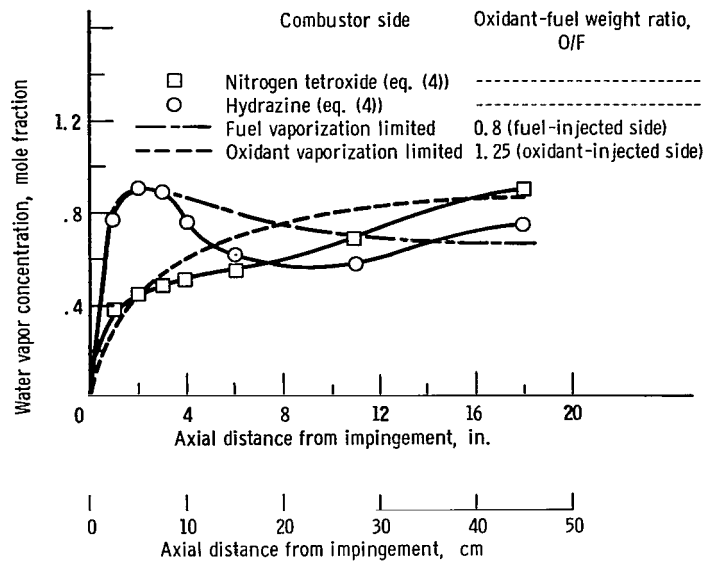


Figure 11. - Comparison of water vapor concentration profiles in combustor. Metered oxidant-fuel weight ratio, 1.0; chamber pressure, 19 atmospheres ( $19.25 \times 10^5 \text{ N/m}^2$ ).

mole fraction  $\text{H}_2\text{O}$  occurred at distances from 2 to 3 inches (5.1 to 7.6 cm) downstream. This maximum results from the relatively high measured radiation at these positions coupled with corresponding low gas temperatures. It is possible that radiation from the 2.2-micron band of  $\text{NH}_3$  may become important near the injector. In that case, the maximum would represent an effect of the hydrazine decomposition reaction as well as an effect of those reactions producing  $\text{H}_2\text{O}$ . On the oxidant-injected sides of the combustor, the mole fraction of  $\text{H}_2\text{O}$  increased continuously with increasing distance.

If the extent of the reaction within the combustor can be assumed to be primarily controlled by the vaporization of one or both propellants, a profile of the  $\text{H}_2\text{O}$  concentration as a function of the axial downstream distance (similar to experimentally derived curves) can be computed. The combustion reaction, if limited by the vaporization of fuel, will proceed at an initially high oxidant-fuel weight ratio. The reverse will be true of oxidant-limited vaporization. Because of the observed stratification of the propellant mixture, the oxidant-injected sides of the combustor were assumed to be limited in oxidant vaporization and to have an overall mixture ratio greater than 1.0; gases on the fuel-injected sides were assumed to be limited in fuel vaporization and to have an overall mixture ratio less than 1.0. Details of this calculation are given in the appendix. Curves showing the best fit to the data are plotted in figure 11. Mole fractions derived from the two sources agree well when the assumptions are considered. Satisfactory data on turbulent mixing are not available for this system, and thus a comprehensive model including both vaporization and mixing effects could not be used.

## CONCLUSIONS

The results of this study showed that the impingement of hydrazine and nitrogen tetroxide resulted in rapid atomization of the liquid jets but did not produce a homogeneous mixture of fuel and oxidant droplets within the chamber. Homogeneous product gases were obtained only by mixing lengths greater than 18 inches (45.7 cm) or by the mixing achieved by longitudinal pressure oscillations.

Gas temperatures derived from uncorrected thermocouple measurements varied from  $300^{\circ}$  K above the fuel decomposition temperature on the fuel-sides of the combustor to  $250^{\circ}$  K below the stoichiometric product temperature on the oxidant-injected sides of the combustor. Relatively constant thermal profiles were established at 11 inches (27.9 cm) or more from the injector.

Spectral radiation intensities of NH, OH, and  $H_2O$  were determined as a function of the axial downstream distance from the injector. Gas temperatures and radiation intensities due to  $H_2O$  were used with Planck's law and a thin gas approximation to calculate the concentration profiles of  $H_2O$  as a function of the axial downstream distance. The resulting curves compared favorably with  $H_2O$  concentrations derived from the extent of combustion as limited by either the fuel or the oxidant vaporization.

Lewis Research Center,  
National Aeronautics and Space Administration,  
Cleveland, Ohio, February 13, 1968,  
128-31-06-03-22.

## APPENDIX - CALCULATION OF WATER VAPOR CONCENTRATION

Calculated water vapor concentrations were derived from combustion profiles based on the vaporization rate of either the fuel or the oxidizer. The percentages of vaporized propellants in the combustor can be related to the combustion efficiency  $\eta$  by the following equation from reference 7:

$$\eta = \frac{(c_{th}^*)_{o/f}}{(c_{th}^*)_{o/f}} \left( \frac{o\dot{w}_o + \mathcal{F}\dot{w}_f}{\dot{w}_o + \dot{w}_f} \right)$$

where

$c_{th}^*$  theoretical characteristic velocity, ft/sec; m/sec

$o/\mathcal{F}$  ratio of vaporized oxidant to vaporized fuel,  $o\dot{w}_o/\mathcal{F}\dot{w}_f$

$o$  percentage of vaporized oxidant

$\mathcal{F}$  percentage of vaporized fuel

$o/f$  metered oxidant-fuel weight ratio,  $\dot{w}_o/\dot{w}_f$

$\dot{w}_o$  liquid-oxidant weight flow, lb/sec; kg/sec

$\dot{w}_f$  liquid-fuel weight flow, lb/sec; kg/sec

With the oxidant vaporization limiting the rate of the reaction, the combustion efficiency can be written

$$\eta = \frac{(c_{th}^*)_{o/f} \frac{o\dot{w}_o}{\dot{w}_f} + 1}{(c_{th}^*)_{o/f} \frac{\dot{w}_o}{\dot{w}_f} + 1}$$

If the fuel limits the rate of the reaction, the efficiency is

$$\eta = \frac{(c_{th}^*)_{o/\mathcal{F}} \frac{\dot{w}_o}{\dot{w}_f} + \mathcal{F}}{(c_{th}^*)_{o/f} \frac{\dot{w}_o}{\dot{w}_f} + 1}$$

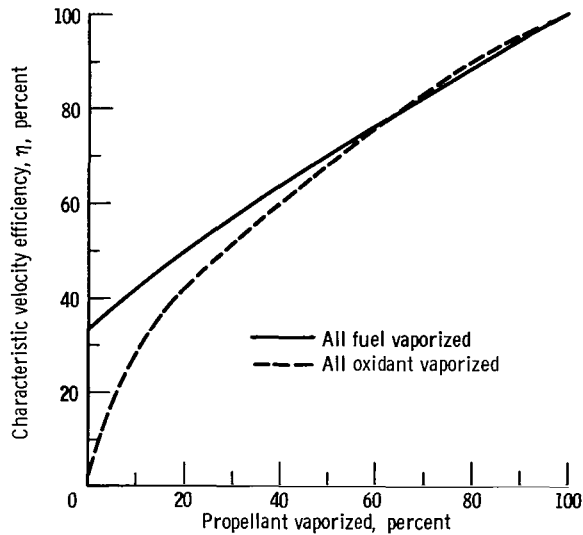


Figure 12. - Vaporization-limited combustion efficiency. Oxidant-fuel weight ratio, 1.0; hydrazine - nitrogen tetroxide system of reference 7.

In reference 11, the variation of the theoretical  $c^*$  over a range of mixture ratios was calculated for equilibrium gaseous products at a chamber pressure of 20 atmospheres ( $20.26 \times 10^5 \text{ N/m}^2$ ). With the use of the equations for the combustion efficiency,  $c^*$  efficiency  $\eta$  was plotted as a function of the percentage of propellant vaporized, as shown in figure 12. Reference 7 also presents a correlation of the generalized chamber length as a function of the propellant vaporized. Within the combustor, the chamber length can be written in the form

$$l_c = l_{\text{gen}} (\eta)^{0.44} (1 - T_{l, o, R})^{0.4} \times \left( \frac{v_m}{0.003} \right)^{1.45} \left( \frac{v_o}{1200} \right)^{0.75} \times \left( \frac{\lambda}{140} \right)^{0.8} \left( \frac{M_a}{100} \right)^{0.35} \left( \frac{P_c}{300} \right)^{-0.66}$$

which, for a chamber pressure  $P_c$  of 20 atmospheres ( $20.26 \times 10^5 \text{ N/m}^2$ ) and a median drop size of 0.003 inch (0.008 cm), reduces to

$$l_c = l_{\text{gen}} (\eta)^{0.44} (1 - T_{l, o, R})^{0.4} \times \left( \frac{v_o}{1200} \right)^{0.75} \left( \frac{\lambda}{140} \right)^{0.8} \left( \frac{M_a}{100} \right)^{0.35}$$

where

$l_c$  chamber length, in.; cm  
 $l_{\text{gen}}$  generalized length parameter

- $\mathcal{A}$  contraction ratio of combustor
- $T_{l, o, R}$  ratio of propellant temperature to its critical temperature
- $v_o$  injection velocity, in./sec; cm/sec
- $\lambda$  latent heat of vaporization, Btu/lb; J/kg
- $\mathcal{M}_a$  molecular weight of propellant, lb mass/lb mole; g/g-mole

For hydrazine, the variation in chamber length with the generalized length parameter becomes  $l_c = l_{gen}(0.65)$  and for nitrogen tetroxide becomes  $l_c = l_{gen}(1.14)$ . The correlation curve in figure 28(f) of reference 7 can be used with the preceding expressions to obtain the variation in chamber length as a function of the vaporized mass of propellant, as shown in figure 13. Since the oxidant vaporization curve is above that of the hydrazine, it is apparent that the combustion in the chamber is limited by the oxidant vaporization to a greater extent than by the fuel vaporization for a given chamber length.

The vaporized propellant can be related to the extent of combustion by calculating the apparent local oxidant-fuel weight ratio as a function of the downstream position. If equilibrium products are assumed at each position, a water vapor concentration can be

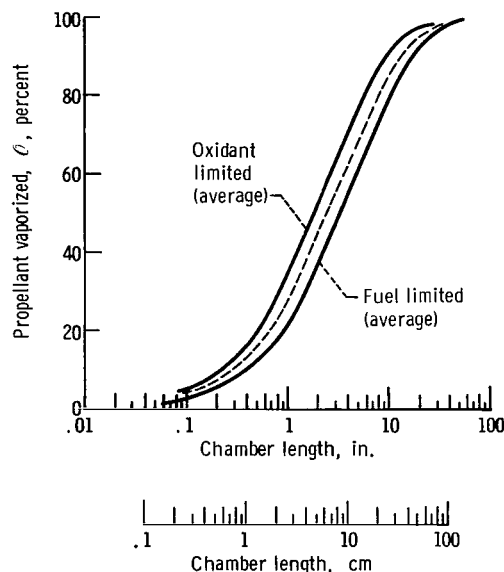


Figure 13. - Vaporization-limited combustion in hydrazine - nitrogen tetroxide system. Median drop size, 0.003 inch (0.008 cm); injection velocity of nitrogen tetroxide (oxidant), 64 feet per second (19.5 m/sec); injection velocity of hydrazine (fuel), 95 feet per second (28.9 m/sec).

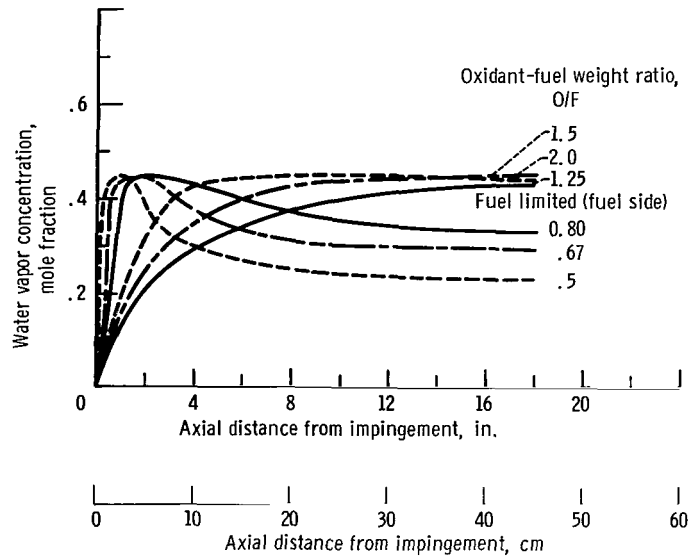


Figure 14. - Calculated water vapor concentration profiles in combustor. Metered oxidant-fuel weight ratio, 1.0; chamber pressure, 19 atmospheres ( $19.25 \times 10^5$  N/m<sup>2</sup>).

calculated for each local mixture ratio. Figure 14 shows various water concentration profiles as a function of the axial distance for a metered oxidant-fuel weight ratio of 1.0. Stratified mixture ratios on the oxidant-injected sides and on the fuel-injected sides of the combustor were, respectively, 2.0 and 0.5, 1.5 and 0.67, and 1.25 and 0.8.

## REFERENCES

1. Rupe, Jack H.: The Liquid-Phase Mixing of a Pair of Impinging Streams. Rep. No. PR 20-195, Jet Propulsion Lab., Calif. Inst. Tech., Aug. 6, 1953.
2. Rupe, Jack H.: A Correlation Between the Dynamic Properties of a Pair of Impinging Streams and the Uniformity of Mixture-Ratio Distribution in the Resulting Spray. Rep. No. PR 20-209, Jet Propulsion Lab., Calif. Inst. Tech., Mar. 28, 1956.
3. Rupe, Jack H.: An Experimental Correlation of the Nonreactive Properties of Injection Schemes and Combustion Effects in a Liquid-Propellant Rocket Engine. Part I: The Application of Nonreactive-Spray Properties to Rocket-Motor Injector Design. Tech. Rep. 32-255 (NASA CR-64635), Jet Propulsion Lab., Calif. Inst. Tech., July 15, 1965.
4. Stanford, H. B.; and Tyler, W. H.: Injector Development. Space Programs Summary No. 37-31, Vol. IV (NASA CR-62607), Jet Propulsion Lab., Calif. Inst. Tech., Feb. 28, 1965, pp. 192-196.
5. Elverum, Gerard W., Jr.; and Staudhammer, Peter: The Effect of Rapid Liquid-Phase Reactions on Injector Design and Combustion in Rocket Motors. Rep. No. PR 30-4, Jet Propulsion Lab., Calif. Inst. Tech., Aug. 25, 1959.
6. Johnson, Bruce H.: An Experimental Investigation of the Effects of Combustion on the Mixing of Highly Reactive Liquid Propellants. Tech. Rep. 32-689 (NASA CR-64616), Jet Propulsion Lab., Calif. Inst. Tech., July 15, 1965.
7. Priem, Richard J.; and Heidmann, Marcus F.: Propellant Vaporization as a Design Criterion for Rocket-Engine Combustion Chambers. NASA TR R-67, 1960.
8. Beltran, M. R.; and Kosvic, T. C.: Parametric Study of Combustion Instability in MMH-NTO Liquid Rocket Engine. Paper No. 66-603, AIAA, June 1966.
9. Skinner, G. B.; Hedley, W. H.; and Snyder, A. D.: Mechanism and Chemical Inhibition of the Hydrazine-Nitrogen Tetroxide Reaction. Monsanto Research Corp. (AFASD-TDR-62-1041), Dec. 1962.
10. Sawyer, Robert F.: The Homogeneous Gas Phase Kinetics of Reactions in the Hydrazine-Nitrogen Tetroxide Propellant System. Tech. Rep. 761 (AFOSR-66-0855, DDC No. AD-634277), Princeton Univ., 1965.
11. Zeleznik, Frank J.; and Gordon, Sanford: A General IBM 704 or 7090 Computer Program for Computation of Chemical Equilibrium Compositions, Rocket Performance, and Chapman-Jouguet Detonations. NASA TN D-1454, 1962.

12. Weiss, Harold G.; Johnson, Bruce; Fisher, H. Dwight; and Gerstein, Melvin: Modification of the Hydrazine-Nitrogen Tetroxide Ignition Delay. AIAA J., vol. 2, no. 12, Dec. 1964, pp. 2222-2223.
13. Eberstein, I. J.; and Glassman, I.: The Gas-Phase Decomposition of Hydrazine and its Methyl Derivatives. Tenth Symposium (International) on Combustion. Combustion Institute, Pittsburgh, 1965, pp. 365-374.
14. Pearse, R. W. B.; and Gaydon, A. G.: The Identification of Molecular Spectra. Third ed., Chapman and Hall, Ltd., London, 1963.

Motion-picture film supplement C-258 is available on loan. Requests will be filled in the order received. You will be notified of the approximate date scheduled.

The film (16 mm, 10 min, color, sound) shows the atomization, mixing, and extent of reaction produced by impinging jets of hydrazine and nitrogen tetroxide, as photographed through transparent and windowed chambers. Distances required to form ligaments and drops near the impingement point are shown. Mixing and the extent of reaction can be determined from the disappearance of oxidizer and the formation of radiating transparent products.

Film supplement C-258 is available on request to:

Chief, Technical Information Division (5-5)  
National Aeronautics and Space Administration  
Lewis Research Center  
21000 Brookpark Road  
Cleveland, Ohio, 44135

CUT

Date

Please send, on loan, copy of film supplement C-258 to  
TN D-4467

Name of Organization

Street Number

City and State

Zip Code

Attention: Mr.  
Title

FIRST CLASS MAIL

OFFICIAL BUSINESS  
FIRST CLASS MAIL  
POSTAGE AND FEES PAID  
NATIONAL AERONAUTICS AND  
SPACE ADMINISTRATION

POSTMASTER: If Undeliverable (Section 158  
Postal Manual) Do Not Return

*"The aeronautical and space activities of the United States shall be conducted so as to contribute . . . to the expansion of human knowledge of phenomena in the atmosphere and space. The Administration shall provide for the widest practicable and appropriate dissemination of information concerning its activities and the results thereof."*

— NATIONAL AERONAUTICS AND SPACE ACT OF 1958

## NASA SCIENTIFIC AND TECHNICAL PUBLICATIONS

**TECHNICAL REPORTS:** Scientific and technical information considered important, complete, and a lasting contribution to existing knowledge.

**TECHNICAL NOTES:** Information less broad in scope but nevertheless of importance as a contribution to existing knowledge.

**TECHNICAL MEMORANDUMS:** Information receiving limited distribution because of preliminary data, security classification, or other reasons.

**CONTRACTOR REPORTS:** Scientific and technical information generated under a NASA contract or grant and considered an important contribution to existing knowledge.

**TECHNICAL TRANSLATIONS:** Information published in a foreign language considered to merit NASA distribution in English.

**SPECIAL PUBLICATIONS:** Information derived from or of value to NASA activities. Publications include conference proceedings, monographs, data compilations, handbooks, sourcebooks, and special bibliographies.

**TECHNOLOGY UTILIZATION PUBLICATIONS:** Information on technology used by NASA that may be of particular interest in commercial and other non-aerospace applications. Publications include Tech Briefs, Technology Utilization Reports and Notes, and Technology Surveys.

*Details on the availability of these publications may be obtained from:*

SCIENTIFIC AND TECHNICAL INFORMATION DIVISION  
NATIONAL AERONAUTICS AND SPACE ADMINISTRATION  
Washington, D.C. 20546